Available online at www.sciencedirect.com
ScienceDirect
Journal of the European Ceramic Society 27 (2007) 3765–3768
www.elsevier.com/locate/jeurceramsoc

Fabrication and characterization of intergrown $Bi_4Ti_3O_{12}$-based thin films using a metal-organic precursor solution

Wataru Sakamoto *, Keiichi Imada, Tetsuo Shimura, Toshinobu Yogo

Division of Nanomaterials Science, EcoTopia Science Institute, Nagoya University, Furo-cho, Chikusa-ku, Nagoya 464-8603, Japan

Available online 12 March 2007

Abstract

Ferroelectric intergrowth-structured $Bi_4Ti_3O_{12}$-based thin films have been fabricated by chemical solution deposition. $Bi_4Ti_3O_{12}$–$SrBi_4Ti_4O_{15}$ (BiT–SBTi) and $SrBi_2Nb_2O_9$–$Bi_4Ti_3O_{12}$ (SBN–BiT) precursor films crystallized in the desired intergrown BiT–SBTi and SBN–BiT structures on $Pt/TiO_x/SiO_2/Si$ substrates by optimizing the processing conditions. Synthesized BiT–SBTi and SBN–BiT thin films exhibited ferroelectric *P–E* hysteresis loops. The BiT–SBTi thin films crystallized at 750 °C showed a $2P_r$ value approximately 20 μC/cm^2. Although a little smaller P_r value was observed for the SBN–BiT thin films, the squareness of a *P–E* hysteresis loop was superior to that of BiT–SBTi thin films. Also, the SBN–BiT thin films had a smoother surface morphology compared with BiT–SBTi thin films.

Keywords: Films; Sol–gel processes; Ferroelectric properties; Titanates

1. Introduction

Recently, rare-earth ion-substituted $Bi_4Ti_3O_{12}$ thin films have been intensively studied to improve the ferroelectric properties of $Bi_4Ti_3O_{12}$ thin films.[1–6] These $Bi_4Ti_3O_{12}$-based thin films have attracted much attention for application in several electronic thin-film devices utilizing ferroelectricity, such as nonvolatile ferroelectric random access memories (NvFeRAMs). However, the fabrication of practical NvFeRAMs is still difficult, because the ferroelectric properties of $Bi_4Ti_3O_{12}$-based thin films are still insufficient compared with those of Pb-based ferroelectric thin films. From such a reason, new thin-film ferroelectrics with excellent ferroelectric properties are strongly demanded.

Bismuth layer-structured ferroelectrics of mixed-layer type[7] have been receiving great attention because of their potential ferroelectric properties. Among several superlattice-structured Bi-based compounds, intergrown $Bi_4Ti_3O_{12}$–$SrBi_4Ti_4O_{15}$ is of interest because of its larger ferroelectricity compared with its constituents $Bi_4Ti_3O_{12}$ and $SrBi_4Ti_4O_{15}$.[8] In the $Bi_4Ti_3O_{12}$–$SrBi_4Ti_4O_{15}$ structure, perovskite blocks of $Bi_4Ti_3O_{12}$ and $SrBi_4Ti_4O_{15}$ are sandwiched between Bi_2O_2 layers and alternatively stacked along the *c* direction in the crystal structure. The lattice mismatch between the perovskite blocks of $Bi_4Ti_3O_{12}$ and $SrBi_4Ti_4O_{15}$ induces a large crystal lattice distortion in the Bi_2O_2 layers, leading to Bi displacement in Bi_2O_2 layers along the direction of polarization. The large ferroelectricity is considered to arise from the Bi displacement in addition to the distortion of perovskite blocks in $Bi_4Ti_3O_{12}$–$SrBi_4Ti_4O_{15}$.[8] The fabrication and electrical characterization of natural-superlattice-structured $Bi_4Ti_3O_{12}$–$SrBi_4Ti_4O_{15}$ thin films have been performed by pulsed laser deposition.[9] However, the synthesis of intergrown $Bi_4Ti_3O_{12}$–$SrBi_4Ti_4O_{15}$ and $Bi_4Ti_3O_{12}$ with other bismuth layer-structured oxide thin films through a chemical route has not been studied up to now.

This paper describes the fabrication and characterization of natural superlattice-structured $Bi_4Ti_3O_{12}$–$SrBi_4Ti_4O_{15}$ and $SrBi_2Nb_2O_9$–$Bi_4Ti_3O_{12}$ thin films on $Pt/TiO_x/SiO_2/Si$ substrates through a chemical solution deposition (CSD). The intergrowth structure, the surface morphology and the ferroelectric properties of synthesized thin films were examined.

2. Experimental procedures

For the preparation of $Bi_4Ti_3O_{12}$–$SrBi_4Ti_4O_{15}$ (BiT–SBTi) and $SrBi_2Nb_2O_9$–$Bi_4Ti_3O_{12}$ (SBN–BiT) precursor solutions, $Sr(OCH(CH_3)_2)_2$, $Bi(OCH_2C(CH_3)_3)_3$, $Ti(OCH(CH_3)_2)_4$ and $Nb(OCH_2CH_3)_5$ [Kojundo Chemical, Japan] were selected as starting materials. 2-Methoxyethanol was dried over molecular sieves and distilled prior to use. The appropriate amounts

* Corresponding author. Tel.: +81 52 789 2751; fax: +81 52 789 2133.
E-mail address: sakamoto@esi.nagoya-u.ac.jp (W. Sakamoto).

0955-2219/$ – see front matter © 2007 Elsevier Ltd. All rights reserved.
doi:10.1016/j.jeurceramsoc.2007.02.041

of $Sr(OCH(CH_3)_2)_2$, $Ti(OCH(CH_3)_2)_4$, $Nb(OCH_2CH_3)_5$ and $Bi(OCH_2C(CH_3)_3)_3$ with 3% excess composition of Bi corresponding to desired compositions were dissolved in 2-methoxyethanol. The solution was refluxed for 20 h to react the starting compounds yielding a brown transparent solution. The entire procedure was performed in a dry nitrogen atmosphere. The precursor solution was concentrated to approximately 0.1 M by removal of the solvent by vacuum evaporation. This solution was stable more than 6 months.

BiT–SBTi and SBN–BiT precursor films were prepared by spin coating on $Pt/TiO_x/SiO_2/Si$ substrates using the precursor solutions. As-deposited precursor films were dried on a hot plate at 150 °C for 5 min and calcined at 350 °C for 10 min by rapid thermal annealing (RTA) at a rate of 100 °C/min in an oxygen flow. Then the calcined films were crystallized at various temperatures for 30 min by RTA at a rate of 180 °C/min. Film thickness was adjusted to 250 nm by repeating the coating/calcining process.

The crystallographic phases of fabricated thin films were identified by X-ray diffraction (XRD) analysis using Cu Kα radiation with a monochromator. The surface morphology of the thin films was observed using an atomic force microscope (AFM). The cross-section of the crystallized thin films was observed using a scanning electron microscope (SEM) and a transmission electron microscope (TEM). The electrical properties of films were measured using a Pt top electrode with a diameter of 0.2 mm deposited by DC sputtering onto the surface of the films followed by annealing at 600 °C for 10 min. The Pt layer of the $Pt/TiO_x/SiO_2/Si$ substrate was used as a bottom electrode. The ferroelectric properties of the films were evaluated using a ferroelectric test system [Toyo Co., FCE-1] at 100 Hz and at room temperature.

3. Results and discussion

3.1. Crystallization of BiT–SBTi and SBN–BiT thin films

In the case of bismuth layer-structured ferroelectric thin films, elemental Bi is known to evaporate while being accompanied with the generation of oxygen vacancies during heat treatment, yielding thin films with a poor ferroelectricity. Therefore, in this study, the amount of excess Bi was determined according to the previous works.[3,10] The amount of excess Bi was set to be 3 mol% to compensate for the loss of Bi during the thin-film fabrication process.

Fig. 1 illustrates XRD profiles of BiT–SBTi and SBN–BiT thin films prepared at 750 °C on $Pt/TiO_x/SiO_2/Si$ substrates. All as-deposited films crystallized as a randomly oriented Bi-layered perovskite single phase without the formation of second phases such as pyrochlore above 650 °C. In this case, in order to clarify the formation of SBN–BiT and BiT–SBTi intergrowth structure, the full crystallization temperature was selected to be 750 °C. The formation of the superlattice-structured BiT–SBTi and SBN–BiT cannot be confirmed from the XRD data above 2θ of 20°, because the XRD profiles above 2θ of 20° in Fig. 1(a) and (b) are almost the same as those of $SrBi_2Nb_2O_9$, $Bi_4Ti_3O_{12}$ and $SrBi_4Ti_4O_{15}$ due to the presence of similar short-range crystal structures. Crystallization in the intergrowth BiT–SBTi and SBN–BiT structure, therefore, was confirmed by identification of magnified XRD patterns from $2\theta = 5°$ to 20°, since crystallization in the similar intergrowth $Bi_4Ti_3O_{12}$–$BaBi_4Ti_4O_{15}$ structure has been confirmed by 0 0 4 and 0 0 5 reflections of the $Bi_4Ti_3O_{12}$–$BaBi_4Ti_4O_{15}$ phase from $2\theta = 5°$ to 15°.[11] The XRD profiles in the 2θ region from $2\theta = 5°$ to 15° of BiT–SBTi and from 5° to 20° of SBN–BiT are shown in Fig. 2(a) and (b), respectively. Distinct diffraction peaks corresponding to their layered structure with a different lattice parameter c were observed. The peaks, particularly 0 0 l (l: odd number), were identified to be the characteristic peaks for intergrown BiT–SBTi and SBN–BiT structures. Furthermore, the peak positions observed for the BiT–SBTi and SBN–BiT thin films in Fig. 2(a) and (b) were consistent with those calculated for the superlattice-structured BiT–SBTi,[7,8] and SBN–BiT,[7] respectively.

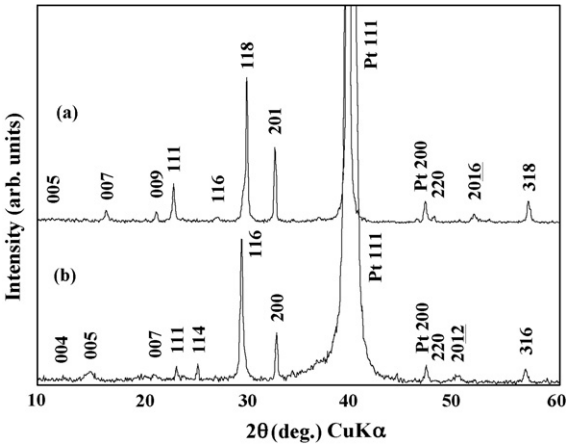

Fig. 1. XRD profiles of (a) $Bi_4Ti_3O_{12}$–$SrBi_4Ti_4O_{15}$ (BiT–SBTi) and (b) $SrBi_2Nb_2O_9$–$Bi_4Ti_3O_{12}$ (SBN–BiT) thin films prepared at 750 °C on $Pt/TiO_x/SiO_2/Si$ substrates.

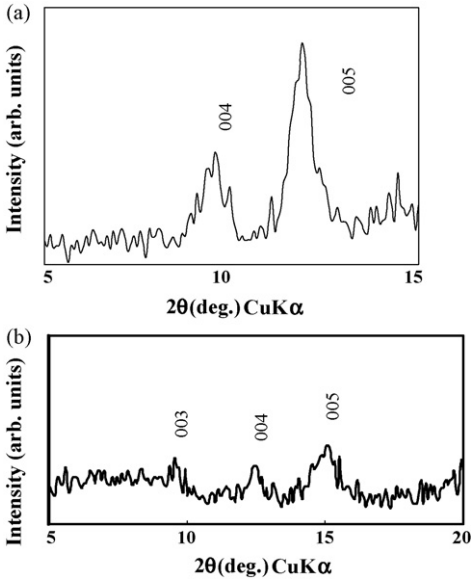

Fig. 2. XRD profiles of (a) BiT–SBTi and (b) SBN–BiT thin films prepared at 750 °C on $Pt/TiO_x/SiO_2/Si$ substrates.

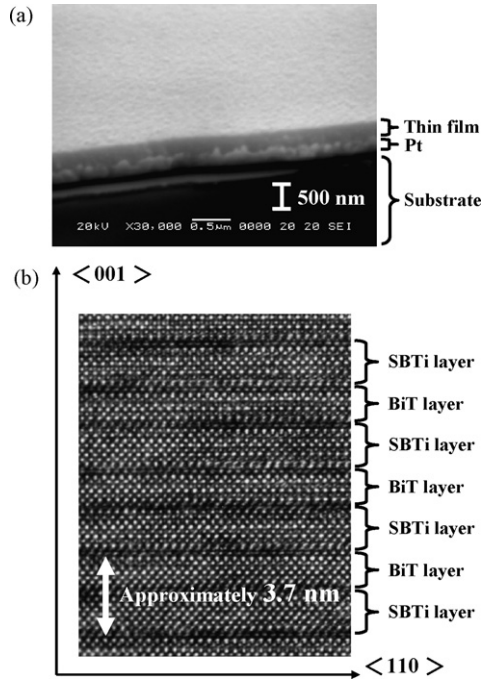

Fig. 3. (a) Cross-sectional SEM image and (b) high-resolution TEM image of BiT–SBTi thin film prepared at 750 °C on Pt/TiO_x/SiO_2/Si substrates.

In order to characterize the microstructure and the lattice image, SEM and TEM observations were also performed for the BiT–SBTi thin film. As can be seen from Fig. 3(a), synthesized BiT–SBTi thin film is crack-free and has a uniform thickness. Moreover, it revealed from the cross-sectional TEM images that no amorphous or second impurity phase was present. A high-resolution TEM (HRTEM) image of the BiT–SBTi thin film is shown in Fig. 3(b). The alternative superlattice stacking of the $Bi_4Ti_3O_{12}$ (BiT) layer and the $SrBi_4Ti_4O_{15}$ (SBTi) layer such as –BiT–SBTi–BiT–SBiTi– was confirmed by the lattice image, where lattice stripes corresponding to the *d*-spacing in the direction of the *c*-axis were observed in the randomly oriented BiT–SBTi thin film. From Fig. 2(b), the length of the BiT–SBTi layer along the *c* direction was found to be approximately 3.7 nm, which was in good agreement with that for BiT–SBTi ceramics measured by XRD.[8] This value is also close to that reported for superlattice-structured BiT–SBTi thin films.[9] However, a small number of defects and discontinuities of the superlattice structures were also found in the BiT–SBTi thin film. The TEM observation of SBN–BiT thin films was also required to confirm the formation of desired intergrowth structure of SBN–BiT, therefore, this is currently under investigation.

3.2. Surface morphology and ferroelectric properties of BiT–SBTi and SBN–BiT thin films

Fig. 4 shows AFM images of BiT–SBTi and SBN–BiT thin films prepared at 750 °C on Pt/TiO_x/SiO_2/Si substrates. The BiT–SBTi thin film consisted of large grains (grain size: approximately 200 nm) with a rough surface (root-mean-square (RMS) roughness: 10.5 nm) and showed an inhomogeneous microstructure. On the other hand, the SBN–BiT thin film exhibited a homogeneous and smooth surface morphology (RMS roughness: 4.3 nm), although it had smaller grains (60 nm) with a relatively uniform and isotropic grain shape compared with that of BiT–SBTi. It reveals from Fig. 4 that the nucleation and growth process of the SBN–BiT and BiT–SBTi thin films is strongly affected by the chemical composition (constituent bismuth layer-structured compounds).

Fig. 5 shows polarization (*P*)–electric field (*E*) hysteresis loops of the BiT–SBTi and SBN–BiT thin films prepared at 750 °C on Pt/TiO_x/SiO_2/Si substrates. The remanent polarization (P_r) and coercive field (E_c) of the BiT–SBTi thin film were 10 μC/cm^2 and 170 kV/cm, respectively. On the other hand, the P_r and E_c of the SBN–BiT thin film were 7.0 μC/cm^2 and 170 kV/cm, respectively. The lower P_r value of the SBN–BiT thin film is ascribed to the microstructure composed of small grains compared to the BiT–SBTi thin film. Although the P_r value of the BiT–SBTi film was larger than that of SBN–BiT, the shape and squareness (P_r/P_s [P_s: saturation polarization]) value

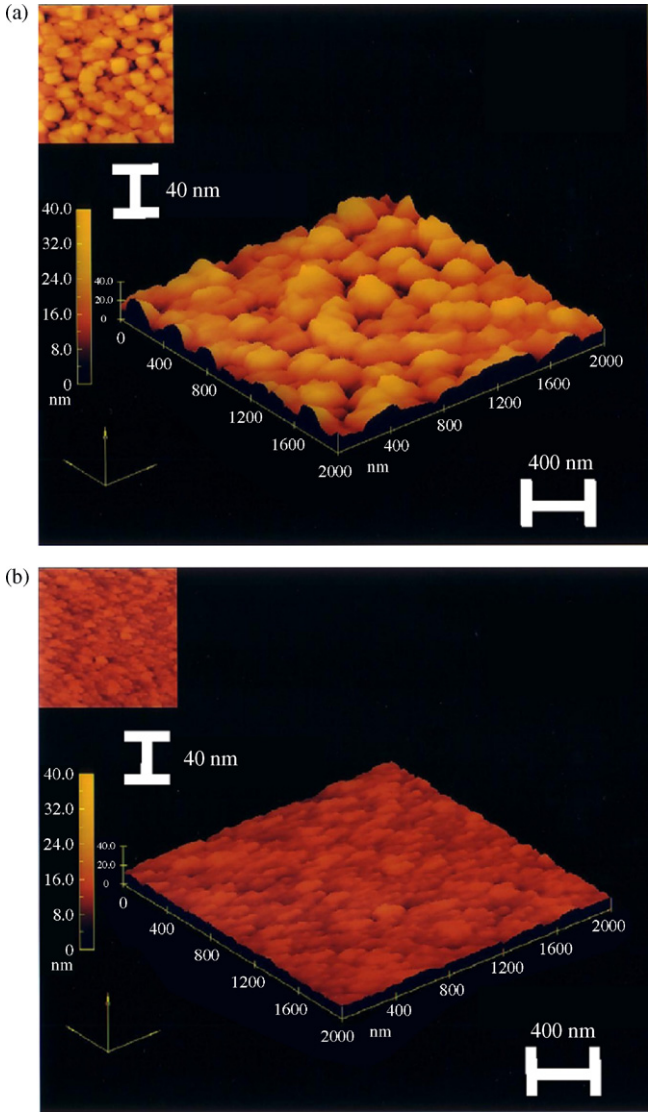

Fig. 4. AFM images of (a) BiT–SBTi and (b) SBN–BiT thin films prepared at 750 °C on Pt/TiO_x/SiO_2/Si substrates.

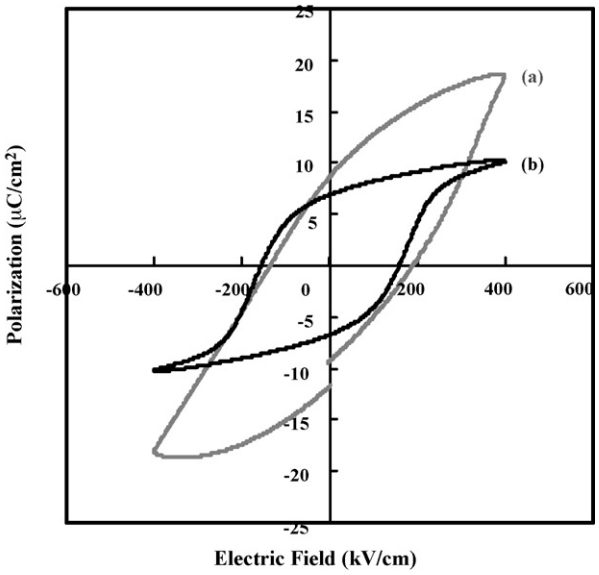

Fig. 5. *P–E* hysteresis loops of (a) BiT–SBTi and (b) SBN–BiT thin films prepared at 750 °C on Pt/TiO_x/SiO_2/Si substrates (measured at 100 Hz and room temperature).

of the SBN–BiT films were superior to those of BiT–SBTi. This good saturation behavior of the SBN–BiT thin film is considered to be attributable to the good surface morphology to apply the electric field uniformly. However, the intergrown BiT–SBTi and SBN–BiT thin films prepared in this study did not show large ferroelectricity. Moreover, the E_c values of these films are still high. In the case of BiT–SBTi and SBN–BiT, these compounds contain volatile Bi ions, particularly in the perovskite blocks, which are easily evaporated during heating. This volatility of Bi ions triggers the formation of oxygen vacancies and affects the grain growth behavior and the ferroelectric characteristics of the resultant thin films. To overcome this problem, Zhu et al. have studied La-substituted BiT–SBTi ceramics.[12] Shibuya et al. demonstrated the ferroelectric properties (P_r: 16 μC/cm^2, E_c: 95 kV/cm) of BiT–SBTi films by PLD.[9] Further optimization of the processing conditions (rare-earth ion substitution,[10] etc.) is required to improve the microstructure and ferroelectric properties. The low-temperature fabrication of the BiT–SBTi and SBN–BiT thin films with controlling the crystal orientation and the evaluation of other electrical properties are also important, and they are now in progress.

4. Conclusions

Intergrown BiT–SBTi and SBN–BiT thin films were successfully synthesized from metalorganic precursor solutions. The synthesized films crystallized into a single phase of desired BiT–SBTi and SBN–BiT structures on Pt/TiO_x/SiO_2/Si substrates. The formation of natural superlattice structure of BiT–SBTi and SBN–BiT was confirmed by characteristic XRD peaks and a HRTEM image. The BiT–SBTi and SBN–BiT thin films exhibited typical ferroelectric *P–E* hysteresis loops. Although the several improvements were required, superlattice-structured BiT–SBTi and SBN–BiT thin films developed in this study might be suitable for applications in several ferroelectric thin film devices, such as NvFeRAMs.

Acknowledgement

This work was supported in part by the Research Foundation for the Electrotechnology of Chubu.

References

1. Park, B. H., Kang, B. S., Bu, S. D., Noh, T. W., Lee, J. and Joe, W., Lanthanum-substituted bismuth titanate for use in non-volatile memories. *Nature*, 1999, **401**, 682–684.
2. Chon, U., Jang, H. M., Kim, M. G. and Chang, C. H., Layered perovskites with giant polarizations for nonvolatile memories. *Phys. Rev. Lett.*, 2002, **89**, 87601-1-4.
3. Hayashi, T., Togawa, D., Yamada, M., Sakamoto, W. and Hirano, S., Preparation and properties of $Bi_{4-x}La_xTi_3O_{12}$ ferroelectric thin films using excimer UV irradiation. *Jpn. J. Appl. Phys.*, 2002, **41**, 6814–6819.
4. Kojima, T., Watanabe, T., Funakubo, H., Saito, K., Osada, M. and Kakihana, M., Ferroelectric properties of lanthanide-substituted $Bi_4Ti_3O_{12}$ epitaxial thin films grown by metalorganic chemical vapor deposition. *J. Appl. Phys.*, 2003, **93**, 1707–1712.
5. Yamada, M., Iizawa, N., Yamaguchi, T., Sakamoto, W., Kikuta, K., Yogo, T., Hayashi, T. and Hirano, S., Processing and properties of rare earth ion-doped bismuth titanate thin films by chemical solution deposition method. *Jpn. J. Appl. Phys.*, 2003, **42**, 5222–5226.
6. Sakamoto, W., Mizutani, Y., Iizawa, N., Yogo, T., Hayashi, T. and Hirano, S., Fabrication and properties of Ge-doped $(Bi,Nd)_4Ti_3O_{12}$ thin films by chemical solution deposition. *Jpn. J. Appl. Phys.*, 2004, **43**, 6599–6603.
7. Kikuchi, T., Watanabe, A. and Uchida, K., A family of mixed-layer type bismuth compounds. *Mater. Res. Bull.*, 1977, **12**, 299–304.
8. Noguchi, Y., Miyayama, M. and Kudo, T., Ferroelectric properties of intergrowth $Bi_4Ti_3O_{12}$–$SrBi_4Ti_4O_{15}$ ceramics. *Appl. Phys. Lett.*, 2000, **77**, 3639–3641.
9. Shibuya, A., Noda, M. and Okuyama, M., Natural-superlattice-structured ferroelectric $Bi_4Ti_3O_{12}$–$SrBi_4Ti_4O_{15}$ thin films prepared by pulsed laser deposition. *Jpn. J. Appl. Phys.*, 2003, **42**, 5986–5989.
10. Sakamoto, W., Imada, K., Shimura, T. and Yogo, T., Synthesis and properties of intergrown $Bi_4Ti_3O_{12}$–$SrBi_4Ti_4O_{15}$ ferroelectric thin films by chemical solution deposition. *Jpn. J. Appl. Phys.*, 2005, **44**, 6952–6956.
11. Kobayashi, T., Noguchi, Y. and Miyayama, M., Polarization properties of superlattice-structured $Bi_4Ti_3O_{12}$–$BaBi_4Ti_4O_{15}$ single crystals and ceramics: comparison with $Bi_4Ti_3O_{12}$ and $BaBi_4Ti_4O_{15}$. *Jpn. J. Appl. Phys.*, 2004, **43**, 6653–6657.
12. Zhu, J., Chen, X.-B., Lu, W.-P., Mao, X.-Y. and Hui, R., Properties of lanthanum-doped $Bi_4Ti_3O_{12}$–$SrBi_4Ti_4O_{15}$ intergrowth ferroelectrics. *Appl. Phys. Lett.*, 2003, **83**, 1818–1820.